Supplementary Information (SI) for Soft Matter.

Electronic Supplementary Information (ESI)

Microrheology of Gemini surfactants at interfaces and in solutions in the dilute and semidilute regimes

Mayssa Medfai,[1] Antonio Stocco,[2] Christophe Blanc,[1] Maurizio Nobili,[1] Martin In[1]

1. Laboratoire Charles Coulomb (L2C), University of Montpellier, CNRS, Montpellier, France

2. Institut Charles Sadron (ICS), University of Strasbourg, CNRS, Strasbourg, France

ESI.1 Surface tension and ellipsometry

The shape of the surface tension curve (Figure 2a in the main text) shows two peculiar features: first, its concavity reverses at a bulk concentration C_1 = 1·10^{-5} mol/L. Second, in the semi-log representation, $\sigma(C)$ appears as a straight line over the last decade of concentrations right below the cmc. At concentrations $C < C_1$, the surface tension decreases linearly with bulk concentration (continuous line in Figure 2a in the main text) and $-\frac{d\sigma}{dC}$ =3.6 N·m^2/mol.

The first few data presented in Figure 2a and corresponding to Henry' regime of adsorption can be adjusted as well with both following equations:

$\sigma = 79.3 - 3.6\cdot10^6\cdot C$ Equation S1

or $\sigma = 72 - 4\cdot10^6\cdot(C - 2\cdot10^{-6})$ Equation S2

with σ in mN/m and C in mol/L.

In this most dilute regime referred to as Henry's regime of adsorption, we assume that surfactant ions and bromide counter-ions adsorb concomitantly so as to build a neutral layer. Consequently, Gibbs equation reads as:[1]

$$\Gamma = -\frac{1}{4RT}\frac{d\sigma}{d\ln C} = -\frac{C}{4RT}\frac{d\sigma}{dC}$$ Equation S3

This leads to Henry's adsorption isotherm $\Gamma = d \cdot C$, where $d = 360$ μm. The Henry's constant d has the dimension of a length and can be interpreted as the thickness of a layer of solution that contains as many molecules as the interface. It characterizes the surface activity of the surfactant: The larger d the stronger the surface activity of the surfactant.

Note that a linear extrapolation of the data to zero concentration leads to a value of surface tension significantly higher (79.3 mN/m) than the one expected for pure water of (72 mN/m). This can be attributed to a small difference between the nominal concentration C and the effective one in the bulk, the latter being lower due to adsorption on all the interfaces that have been in contact with the sample. Such difference of C has been reported for high molecular weight surface active compounds such as polymers or proteins which are studied at quite low molar concentration.[2] In our data the reduction of the effective concentration is also suggested by the peculiar shape of the curve in Figure 2a, which shows an upward concavity in an intermediate range of concentration around 10^{-5} mol/L.

Alternatively, the difference of the surface tension (79.3 and 72 mN/m) can be attributed to Langmuir's cohesive pressure, as has been shown by Ivanov's group and others.[3] Cohesive pressure for our charged surfactant as trimers may result from the spacer (in fact a linker) acting as a very effective factor of cohesion between the amphiphilic moieties.

For $C_1 < C <$ cmc, the surface tension of the solutions decreases logarithmically with the concentration and $-\frac{d\sigma}{d\ln c} = 4.6$ mN/m.

The concentration dependence of the surface tension can be fitted by the following equation (dashed line in Figure 2a):

$$\sigma = -13.6 - 4.6 \cdot \ln(C - 7.1 \cdot 10^{-6}),$$ Equation S4

where a concentration term $7.1 \cdot 10^{-6}$ mol/L has been added (higher than the one applied at low concentration), which allows satisfying continuity with the low concentration linear regime in terms of surface tension and its derivative.

According to Equation S3 and S4, Γ gets constant at a concentration one order of magnitude lower than the cmc. The question of the concomitance of interface saturation and cmc has been scrutinized using neutron reflectivity for non-ionic, anionic and cationic surfactants.[2,4,5] The answer varies upon the type of surfactants: for non-ionic surfactants the adsorption limit is reached below the cmc, while for several ionic ones saturation is not reached at the cmc. The ellipsometry data presented in Figure 2b in the main text confirm this conclusion. Surface excess concentration shows saturation only at the cmc. The change of concavity of the concentration dependence of the surface tension might rather be due to the polyelectrolyte nature of trimer surfactants which could induce partial bromide ions condensation on non-micellized surfactant ions or to its high content in aliphatic chains which could lead to premicellization.[1,2,6] This makes the approximation of activities by concentrations less reliable in this range of concentrations and could explain the peculiar shape of the graph of $\sigma(C)$ right before cmc.[7]

Figure 2b (in the main text) presents the surface excess concentration Γ obtained by ellipsometry as a function of the bulk concentration. For C < cmc, Γ can be fitted with a Langmuir isotherm up to the cmc:

$$\boldsymbol{\Gamma} = \frac{\mathbf{0.43}\boldsymbol{C_{eff}}}{\mathbf{1+2.5\cdot 10^5}\boldsymbol{C_{eff}}} \qquad \text{Equation S5}$$

where $C_{\text{eff}} = C - 1.2 \cdot 10^{-6}$ (in mol/L). Equation S5 corresponds to the dashed line in Figure 2b (in the main text). At low concentrations, $\Gamma/C \approx 430$ μm, consistent with our analysis of the surface tension results in the early stage of adsorption.

Adsorption regime ends up at the cmc and both methods of surface tension measurements yield cmc consistent with the one obtained from conductimetry, between 1.3 and $1.7\cdot10^{-4}$ mol/L.[7] The surface tension data show a shallow minimum usually associated with the presence of minute amounts of apolar surface active impurities that get solubilized beyond cmc.

Hence, from the surface activity of the 12-3-12-3-12, 3Br we can estimate its free energy of adsorption at air-solution interface. At low concentration both tensiometry and ellipsometry allow to characterize the surface activity by a length $\frac{d\Gamma}{dC} = d \approx 400\mu\text{m}$ ±10%. This length corresponds to the Henry's constant, it means the proportionality factor between bulk concentration and surface excess concentration, at the early stage of adsorption. For the trimeric surfactant under scrutiny, it is much larger than the one characterizing the

monomeric analog DTAB and the dimeric surfactant 12-3-12, 2Br or 12-2-12, 2Br. Using data from literature we found $d \approx 1$ μm for DTAB, $d \approx 12$ μm for 12-3-12, 2Br and $d \approx 18$ μm for 12-2-12, 2Br.[8,9] Interestingly, the length d can be interpreted as the thickness of a layer of the bulk solution that contains as many molecules as the interface. For a Langmuir monolayer of insoluble surfactant, $d \to \infty$. The standard free energy of adsorption per surfactant ΔG^0 defined as the difference in standard chemical potential in the bulk and at interface is given by the ratio of concentrations in the bulk and in the interfacial region according to Boltzman principle:

$$\exp\left(-\frac{\Delta G^0}{k_B T}\right) = \frac{C_{interface}}{C_{bulk}} = \frac{l_m}{d}, \qquad \text{Equation S6}$$

l_m = 2 nm is the thickness of the interfacial layer taken that we approximate as the largest molecular dimension of the C_{12} surfactant as given by Tanford.[10] We calculate ΔG^0=12 $k_B T$ per molecule of 12-3-12-3-12, 3Br (30 kJ/mol), compared to 6 $k_B T$ (15 kJ/mol) for DTAB and 9 $k_B T$ (22 kJ/mol) for the dimers. It is worth noting that the value obtained for the dimers is the same as the one obtained for 12-2-12, 2 2Br from a fitting of the complete isotherm and taking into account electrostatic interactions.[9] This comparison supports our approach which amounts to considering the adsorption at air-water interface in its earliest stage as an isothermal compression of a perfect gas.

Beyond cmc, the surface tension decreases much less as the concentration increases. This is expected due to the much weaker concentration dependence of the chemical potential of surfactants when they micellize. For $2 \cdot 10^{-4} < C < 10^{-2}$ mol/L, surface tension decreases logarithmically from 32 mN/m down to 30 mN/m, with $-\frac{d\sigma}{dlnC} = 0.6$ mN/m. For the three highest measured concentrations, the surface tension drops further. The lowest value measured at $7 \cdot 10^{-2}$ mol/L (500 cmc) is 24 mN/m. Very few studies have been devoted to the evolution of surface tension of concentrated surfactants solution well above cmc. A noticeable one reports on the decrease of surface tension at C = 8 cmc concomitantly with a morphological transition of sodium dodecyl sulfate micelles from spheres to rods induced by addition of aluminum cations.[11] Noteworthy, the aggregation number of the micelles does not enter explicitly in the proposed model for surface tension. The decrease of surface tension above cmc is actually not

directly due to the elongation of the micelles from spheres to rods but is a consequence of a selective enhancement of counterions condensation as micelles grow.[9]

ESI.2 Refractive index increment

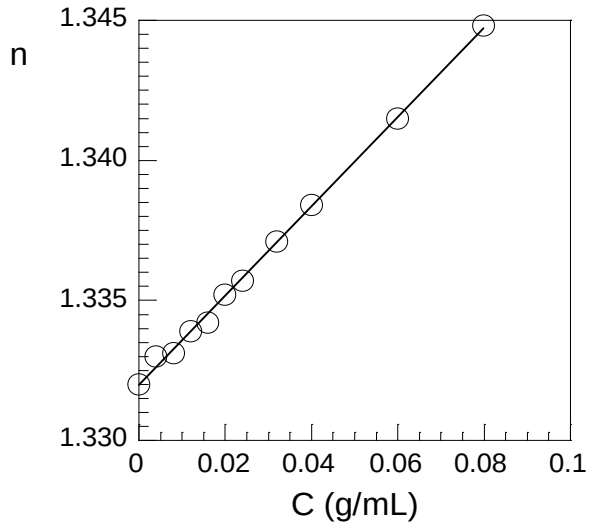

Figure S1: Refractive index of aqueous solutions of 12-3-12-3-12, 3 Br surfactant versus concentration. Equation of best linear fit reads : $\boldsymbol{n = 1.332 + 0.159 \cdot C}$, with $\boldsymbol{R^2 = 0.998}$.

ESI.3 Experimental error on the diffusion coefficient measurements

Relative experimental errors on diffusion measurements are shown in Figure S2.

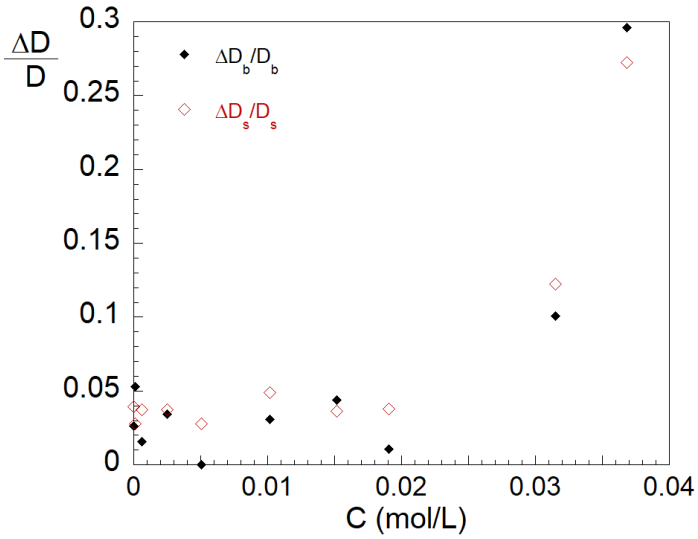

Figure S2 : Relative experimental error made on the determination of the bulk and the interfacial diffusion coefficients.

Even for the highest concentrations in the bulk, our MSD data probe only the viscosity of the solution. To check the impact of the viscoelasticity on our data, we calculated MSD as a function of the lag time as it is explained in the following.

We considered the viscoelastic properties of our gemini surfactant solution at 3.7 10^{-2} mol/L (2.5 %), which have been measured in the linear regime of the dynamic mode of shearing, see Figure S3 left.[12] This concentration has been chosen because it corresponds to a zero shear viscosity of 2.1 Pa.s close to the viscosity of the highest concentration studied in this work. It is characterized by relaxation time of 0.12 s. Figure S3 right shows the calculated MSD of a particle diffusing in a Maxwellian fluid with the same relaxation time and the same viscosity. It presents a plateau at short time due to the elastic properties of the solution and crosses over to a diffusive regime at longer time. In our experiment, this plateau is not accessible due to limited spatial resolution which leads to an error on the localization of the particle. Including this localization error in the calculation (open symbols) shows that the apparent time of the onset of diffusive regime is shifted so that we cannot access the rheological time with our setup.

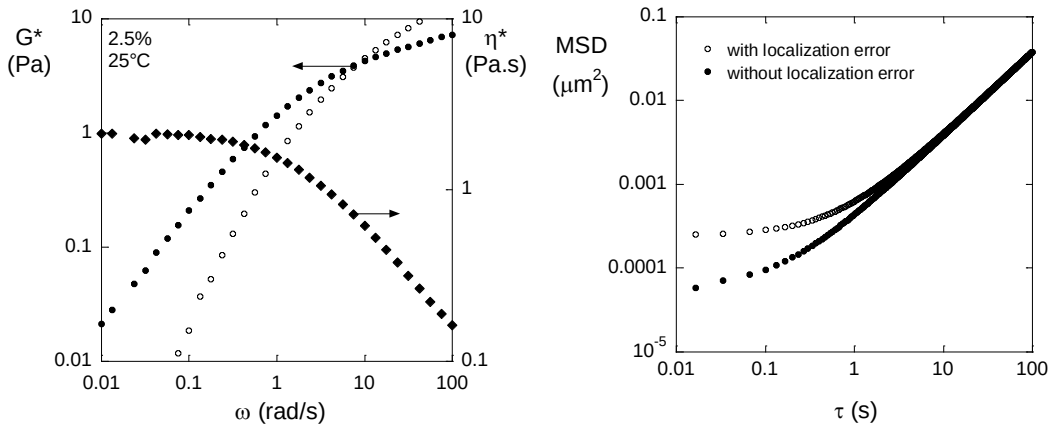

Figure S3: (left) Complex shear modulus G^* and viscosity as a function of the frequency of a 3.7 10^{-2} mol/L (2.5%) gemini surfactant solution. (right). Calculated MSD in a Maxwell fluid showing the same viscoelasticity as shown on the left plot.

ESI.4 Particle contact angle as a function of the concentration

Particle contact angle changes only in the adsorption regime, going from 54°± 5° at pure water interface down to 37 ± 5 ° and remains constant beyond the cmc, see Figure S4. The contact angle depends on the interfacial energies γ involved at the triple contact line and reads: $\gamma_{sv} - \gamma_{sl}=\cos(\theta)\sigma$, where γ_{sv} is the particle-air surface tension, γ_{sl} is the particle-solution surface tension. Assuming a constant γ_{sv} leads to inverse proportionality between the cosine of the contact angle and σ. So that a decrease of surface tension of the solution leads to a decrease of the contact angle consistent with observation.

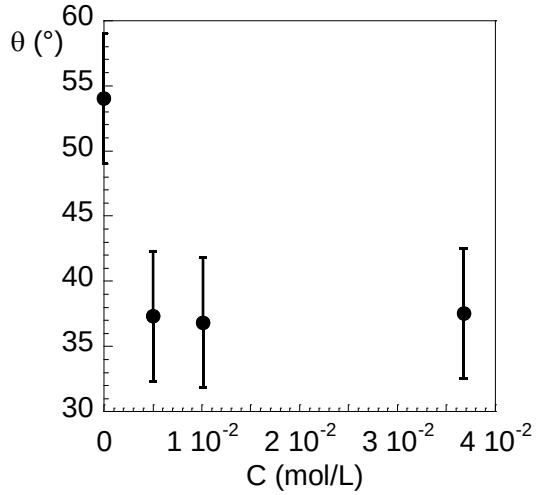

Figure S4: Contact angle of the particle versus bulk concentration.

ESI.5 Microrheology of the bulk solutions

The bulk viscosity $\eta_{b,\mu} = \frac{k_B T}{6\pi D_b R}$ has been determined from the diffusion of the same type of particles measured at the interface. The bulk viscosity first increases linearly with surfactant concentration, see insert of Figure S5. Analyzing this linear increase with Einstein formula for the viscosity $\eta_b = \eta_0(1 + 2.5\Phi)$, where Φ is the volume fraction, yields an average hydrodynamic radius of the micelles equal to 2.3 nm (corresponding diffusion coefficient of 94 $\mu m^2/s$), consistent with small angle neutron scattering measurements of the radius R = 1.8 nm. For $C > 4 \cdot 10^{-3}$ mol/L = 50 cmc the increase in viscosity with concentration steepens and the viscosity increases by more than three orders of magnitude in less than a decade of concentration. This steep increase of bulk viscosity is the rheological signature of the shape transition of micelles from spheres to wormlike, but it is worth noting that it occurs a decade of concentration higher than the shape transition observed by scattering techniques (see Figure 3 of the main text).

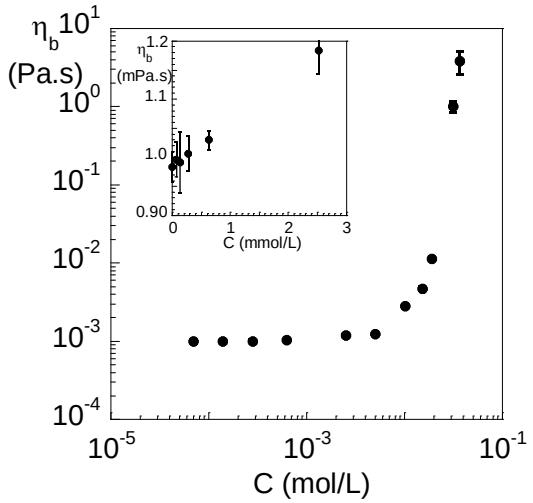

Figure S5 : Bulk viscosity, from microrheology, versus concentration as deduced from the bulk diffusion coefficient. Inset shows the initial linear increase of viscosity in linear scale, the slope of which being related to the volume fraction of the micelles.

ESI.6 Relation between the reduced drag coefficients and interfacial shear viscosity

According to Fischer:[13] $\zeta_s = f_s \eta R$ where $f_s \approx f^{(0)} + f^{(1)} Bo$ at low Boussinesq number Bo.

$$\Delta\zeta^R = \zeta_s^R - \zeta_b^R = \frac{\zeta_s}{\zeta_{so}} - \frac{\zeta_b}{\zeta_{bo}} \qquad \text{Equation S7}$$

$$\Delta\zeta^R = \frac{f^{(0)}\eta R + f^{(1)} Bo\, \eta R}{\zeta_{so}} - \frac{\eta}{\eta_0} \qquad \text{Equation S8}$$

Since $\frac{f^{(0)}\eta R}{f_0{}^{(0)}\eta_0 R} \approx \frac{\eta}{\eta_0}$,

$$\Delta\zeta^R \approx \frac{f^{(1)} Bo\, \eta R}{\zeta_{so}} = \frac{\eta_s f^{(1)}}{\zeta_{so}} \frac{R}{l_c} = \frac{\eta_s f^{(1)}}{f_0{}^{(0)}\eta_0 R} \frac{R}{l_c} = \frac{f^{(1)}}{f_0{}^{(0)}\eta_0 l_c} \eta_s \qquad \text{Equation S9}$$

References

1 J. Wegrzynska, G. Para, J. Chlebicki, P. Warszynski and K. Wilk, *Langmuir*, 2008, **24**, 3171–3180.

2 P. X. Li, Z. X. Li, H.-H. Shen, R. K. Thomas, J. Penfold and J. R. Lu, *Langmuir*, 2013, **29**, 9324–9334.

3 R. I. Slavchov, I. M. Dimitrova and I. B. Ivanov, *Underst. Complex Syst.*, 2013, 199–225.

4 L. Lee, O. Guiselin, A. Lapp, B. Farnoux and J. Penfold, *Phys. Rev. Lett.*, 1991, **67**, 2838.

5 I. Tucker, J. Penfold, R. K. Thomas and D. J. Tildesleyt, *Langmuir*, 2009, **25**, 3924–31.

6 C. M. Phan, C. V. Nguyen, H. Nakahara, O. Shibata and T. V. Nguyen, *Langmuir*, 2016, **32**, 12842–12847.

7 P. X. Li, C. C. Dong, R. K. Thomas, J. Penfold and Y. Wang, *Langmuir*, 2011, **27**, 2575–2586.

8 V. E. Cuenca, M. Fernández Leyes, R. D. Falcone, N. M. Correa, D. Langevin and H. Ritacco, *Langmuir*, 2019, **35**, 8333–8343.

9 V. Bergeron, *Langmuir*, 1997, **7463**, 3474–3482.

10 C. Tanford, *Proc. Natl. Acad. Sci. U. S. A.*, 1979, **76**, 4175–6.

11 R. G. Alargova, K. D. Danov, J. T. Petkov, P. A. Kralchevsky, G. Broze and A. Mehreteab, *Langmuir*, 1997, **13**, 5544–5551.

12 M. In, G. G. Warr and R. Zana, *Phys. Rev. Lett.*, 1999, **82**, 2278–2281.

13 T. M. Fischer, P. Dhar and P. Heinig, *J. Fluid Mech.*, 2006, **558**, 451–475.